

# FDTD MODELING OF REFRACTOMETRIC OPTICAL SENSORS BASED ON QUASI-ONE-DIMENSIONAL PHOTONIC CRYSTALS

G. S. Kliros and K. A. Papageorgiou

*Hellenic Air-Force Academy, Department of Aeronautical Sciences  
Division of Electronics and Communication Engineering  
Dekeleia Air-Force Base, Attica GR-1010, Greece  
gksma@hol.gr*

## Abstract

*We report on the design of a refractometric optical sensor based on a quasi-one dimensional photonic crystal structure etched in a  $\text{Si}_3\text{N}_4$  ridge waveguide grown on top of a  $\text{SiO}_2$  substrate. A photonic crystal based on this kind of structure exhibits a photonic bandgap for TE polarized light. The finite difference time domain method (FDTD) is employed in order to design the device and investigate its transmission spectra and sensitivity characteristics. The shift in the central wavelength of the reflectivity spectrum, due to change in the refractive index, when the low-index areas of the photonic crystal are infiltrated with different fluids, is found to be linear and hence, suitable for refractometric sensing applications.*

## 1. INTRODUCTION

Integrated optical sensors has a high potential to be employed as a device in many areas such as, microbiology, environmental safety, defence and aerospace technology. Their main advantages are immunity to electromagnetic interference, high compactness and robustness and prospects of mass production, and also they have fast responsivity and higher sensitivities when compared to Micro-Electro-Mechanical Systems (MEMS). In a variety of environmental, biomedical and aerospace applications, the measurement of the refractive index is very important since is strongly related to structure composition.

Photonic crystals (PC) and photonic band gap structures (PBG) [1] are very promising building blocks for photonic components of submicron scale which is comparable to that of their electronic counterparts. Two-dimensional (2D) PCs formed in a dielectric slab waveguide structure have attracted much interest recently for realizing novel micro-optoelectronic devices [2-4]. A structure having a periodic index modulation in one dimension is known as a one-dimensional photonic crystal (1D-PC). If the structure has nonperiodic features in the other two dimensions, it is denoted as a quasi-1D PC which is essentially a 'Bragg grating'. A Bragg grating with a strong index modulation shows a typical property of PCs: an extended transmission stop-band. The width of this stopband and the steepness of its edges increase with the strength of the refractive index modulation. For sensing appli-

cations, one has to exploit the steep edges of the stop-band in a strong grating [5].

In this paper, motivated by the recent interest in developing quasi-1D PC sensors [6,7], we designed and simulated a wide ridge-type channel waveguide of silicon nitride with a 1D PC etched into the core layer. The reflectivity spectra of the device has been obtained using the FDTD method. The sensitivity of our device is determined by observing the shift in the central wavelength of reflectivity spectrum as a function of the change in effective refractive index.

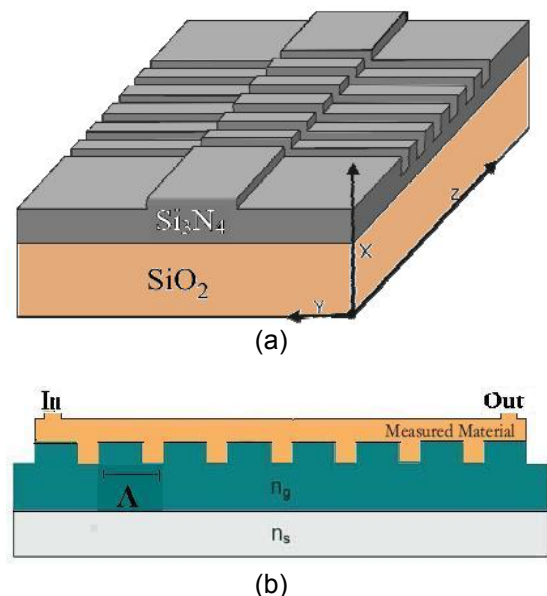


**Fig.1.** (a) Schematic 3D drawing of the waveguide with a 1D photonic crystal, and (b) Cross-section of the quasi one-dimensional photonic crystal sensor with a cuvette placed on top.

## 2. DEVICE DESIGN AND MODELING

A schematics of the 3D-structure as well as the cross-section of the device is shown in Fig.1. The sensing element is a strong grating in a  $\text{Si}_3\text{N}_4$  ridge waveguide ( $n_g=2.01$ ) with period  $\Lambda=628.2$  nm grown on top of a  $\text{SiO}_2$  substrate ( $n_s=1.46$ ) resulting in TE single-mode operation at wavelengths around the modern telecommunications wavelength of  $\lambda=1.55$   $\mu\text{m}$ . The light is guided by the photonic crystal structure in the horizontal plane and is confined by the classical ridge waveguide in the vertical direction. The sensitivity of the sensor for changes in the refractive index can be simulated by infiltrating the grooves of the grating with different fluids through the cuvette, as it is shown schematically in Fig. 1(b).

The simulation is performed using the Finite Difference Time Domain Method (FDTD) with Perfectly Matched Layer (PML) boundary conditions. Since the waveguide thickness is very small and there is no structural variation in the y-direction uniformly over the x-z plane, the structure can be analysed as a quasi-1D device without losing much generality. FDTD method relies on the discretization of Maxwell's equations and provides the description of the time evolution of the electromagnetic field without any assumption about the number and the characteristics of the propagating modes.

According to FDTD method on a Yee cell [8], a simple set of discrete field equations is obtained for TE-polarized wave propagation:

$$\begin{aligned} E_x^{n+1}(i) = E_x^n(i) + \frac{\Delta t}{\epsilon(i)\Delta z} \times \\ \times \left[ H_y^{n+\frac{1}{2}}(i+1/2) - H_y^{n+\frac{1}{2}}(i-1/2) \right] \end{aligned} \quad (1)$$

$$\begin{aligned} H_y^{n+\frac{1}{2}}(i+1/2) = H_y^{n-\frac{1}{2}}(i+1/2) + \\ + \frac{\Delta t}{\mu(i)\Delta x} [E_x^n(i+1) - E_x^n(i)] \end{aligned} \quad (2)$$

where  $\Delta t$  and  $\Delta x$  are the finite difference cells in the temporal and spatial domain, respectively. A 1D-mesh grid with size of  $\Delta x=12.035$  nm were used in the simulation. The time step is based on the Courant's condition  $\Delta t = \Delta x / \sqrt{2}c$ , where  $c$  is the velocity of light in vacuum. The simulation is run for 131.072 ( $2^{17}$ ) time steps to get a fine spectral resolution. Vector-based computations are employed instead of element-based ones using MATLAB tech-

nical language in order to reduce the computation time considerably. The source employed was a Gaussian modulated continuous wave at central wavelength of 1.55  $\mu\text{m}$  having a broad spectral bandwidth. By Fast-Fourier-Transforming the electric field component, sampled at the output ports, the frequency response of the device under investigation was obtained, with just a single simulation run.

In order to get an exact Bragg wavelength from the FDTD simulation, the effective index corresponding to TE-mode propagating in the ridge waveguide, is set to a value which is obtained from a Beam Propagation Method (BPM) mode solver [9]. For first-order gratings like in Fig. 1(b), the Bragg conditions are expressed as

$$\Lambda_{\text{tooth}} = \frac{\lambda_{\text{Bragg}}}{4n_{\text{eff,tooth}}}, \quad \Lambda_{\text{groove}} = \frac{\lambda_{\text{Bragg}}}{4n_{\text{eff,groove}}} \quad (3)$$

For the desired Bragg wavelength of 1.55  $\mu\text{m}$ ,  $\Lambda_{\text{tooth}}=240.7\text{nm}$  and  $\Lambda_{\text{groove}}=387.5$  nm so that a grating period  $\Lambda= 628.2$  nm, is obtained. The number of periods chosen was 64, resulting in an overall grating length of 40.2  $\mu\text{m}$ .

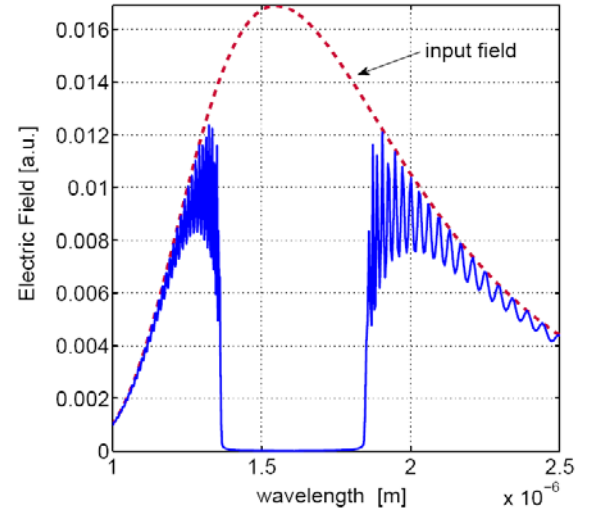


**Fig. 2.** Spectral dependence of the electric field intensity when the grooves are filled with air. The dashed line represents the spectral dependence of the input pulse.

## 3. RESULTS AND DISCUSSION

Fig. 2 shows the spectral intensity of both the input and the transmitted electric field for air-filled grooves. The wide stop band in the transmission spectrum would allow a high free spectral range, so that the Bragg wavelength can be tuned over a

wide range of wavelengths. Table I reports the shift of the central wavelength when the grating grooves are infiltrated by different fluids with increasing refractive indices. Experimentally, a continuous change in refractive index could be realized by mixing together two fluids with different indexes. As it is seen, the central wavelength i.e. the wavelength exactly in the middle of the stopband defined by the -3 dB point of the stopband edges, is shifted towards higher wavelength values as a consequence of the change of the guided mode effective index. Figs. 3(a)-(c) illustrate the effect of fluid refractive index change on the reflectivity of the quasi-1D photonic crystal structure. Both edges of the stopband are shifted toward longer wavelengths. A small wavelength shift of such an edge can cause a large change in the transmitted power from a source having an appropriate wavelength.

Grating sensitivity describes the device efficiency when it works as a sensor. In this work, we define the sensitivity as

$$S = \frac{\partial \lambda_{\text{centre}}}{\partial n_c} \quad (4)$$

and therefore, it can be easily calculated using the data of Table I.

Table I: Resonance central wavelength for different refractive indices

$n_c$	$\lambda_{\text{low}}$ (nm)	$\lambda_{\text{high}}$ (nm)	$\lambda_{\text{centre}}$ (nm)
1.00	1356.7	1857.8	1607.2
1.05	1409.6	1874.8	1642.2
1.10	1466.4	1881.4	1673.9
1.15	1520.2	1896.0	1708.1
1.20	1576.0	1912.0	1744.0
1.25	1631.5	1929.7	1780.6
1.30	1687.3	1944.4	1815.9
1.35	1749.5	1956.4	1852.9
1.40	1806.5	1974.8	1890.7
1.45	1863.2	1993.9	1928.5
1.50	1921.0	2013.5	1967.3

Fig. 4 presents the central wavelength shift ( $\Delta \lambda_{\text{centre}}$ ) as a function of the change in fluid refractive index by infiltration of the grating grooves, where the reference wavelength is the central wavelength for air-filled grooves. From the graph, it is observed a 7 nm shift of the centre wavelength for a change in refractive index  $\delta n_c = 0.1$  and therefore an average sensitivity  $S \sim 70$  nm per unit refractive index change is obtained. Furthermore, the central wavelength shift is linear and hence, the device is extremely suitable for sensing applications.

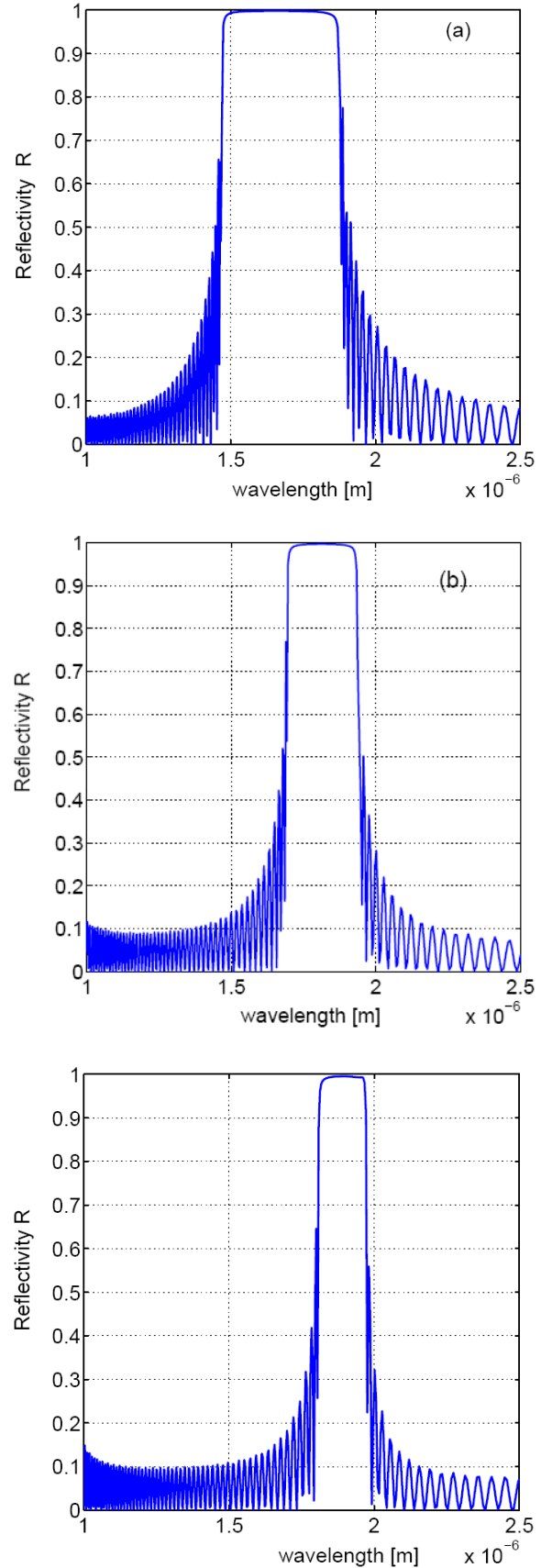


Fig. 3. Computed reflectivity spectra when the refractive index of infiltrated grating grooves is (a)  $n_c=1.1$ , (b)  $n_c=1.3$  and (c)  $n_c=1.4$

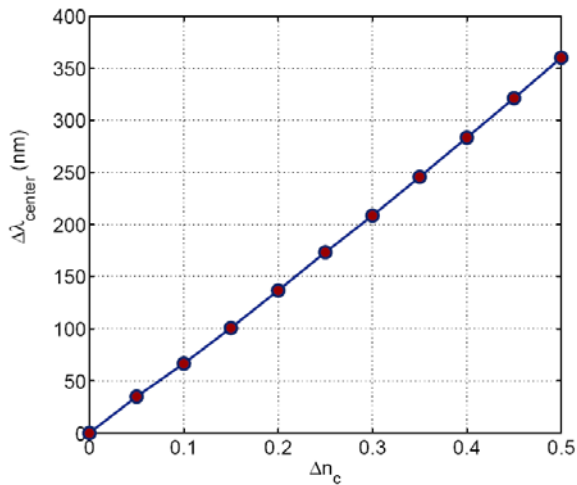


Fig. 4. Sensitivity characteristic curve showing the simulated changes in central wavelength versus changes in refractive index.

#### 4. CONCLUSION

We have designed and simulated a very compact refractometric sensor based on quasi-1D photonic crystal. The FDTD simulation method is employed, in order to investigate its transmission spectra and sensitivity characteristics. For the working wavelength of  $\sim 1.55 \mu\text{m}$ , the transmission spectra has been calculated by changing the refractive index of different fluids in the grooves of the grating. It has been found that increasing the refractive index, the wavelength position of both the lower and upper band edge are shifted with the largest shift appeared in the lower wavelength band edge. The shift in the central wavelength is found to be approximately linear and hence, the device is extremely suitable for sensing applications. The simulated structure shows good performance in terms of compactness, sensitivity and free spectral range. The performance of the designed device as temperature, pressure or strain sensor based on the

thermo-elastic and thermo-optic effects [10] will be reported in a future paper.

#### References

- [1] P. Markos and C. M. Soukoulis, *Wave Propagation: From Electrons to Photonic Crystals and Left-handed Materials*, Princeton University Press, New Jersey, 2008.
- [2] R. V. Nair and R. Vijaya, Photonic crystal sensors: An overview, *Progress in Quantum Electronics*, vol. 34, 2010, pp. 89-134.
- [3] G. S. Kliros, A. N. Fotiadis, G. P. Tziopis, Optical Simulation of Silicon-Based Complete Photonic Bandgap Modulator, *Proc. of 21<sup>th</sup> IEEE Int. Conference on Microelectronics*, Marrakesh, Morocco, 2009, pp. 219-221.
- [4] G. Kliros, K. Papageorgiou, Refractometric Optical Sensor based on Tapered Photonic Crystal Waveguide, *J. Optoelectronics Adv. Mater.*, vol.12 (7), 2010, pp. 1530-1533.
- [5] W. C. L. Hopman *et. al.*, Quasi-1D Photonic Crystal as a Compact Building-Block for Refractometric Optical Sensors," *IEEE J. Sel. Top. Quant. Electron.* vol. 11, 2005, pp. 11–16.
- [6] V. M. N. Passaro *et. al.*, Design of Bragg Grating Sensors Based on Sub-micrometer Optical Rib Waveguides in SOI, *IEEE Sensors J.* vol. 8, 2008, pp.1603-1611.
- [7] A. Banerjee, Binary number sequence multilayer structure based on refractometric optical sensing element, *J. Electromagn. Waves Appl.*, vol. 22, 2008, pp. 2439 - 2449.
- [8] A. Taflove, *Computational Electrodynamics: The Finite-Difference Time-Domain Method*, 2<sup>nd</sup> edn., Artech House, 2000.
- [9] Em. E. Kriezis *et. al.*, Full vector beam propagation method for axially dependent 3-D structures *IEEE Trans. Magnetics*, vol. 33 (2), 1997, pp. 1540-1543.
- [10] H. M. Chong, R. De La Rue, Tuning of photonic crystal waveguide microcavity by thermo-optic effect, *IEEE Photon. Techn. Lett.*, vol. 16 (6), 2004, pp. 1528-1530.